Time harmonic and static crack problems in 3-D transversely isotropic bodies

M. Solis, M. P. Ariza & J. Dominguez
Escuela Superior de Ingenieros, Universidad de Sevilla, Spain

Abstract

Three dimensional crack problems in transversely isotropic solids under static and time harmonic dynamic loading conditions are studied in this paper using a mixed BE approach. Hypersingular and strongly singular kernels appearing in the formulation are regularized prior to any discretization. Two different crack geometries are studied. Stress Intensity Factors are computed from the crack opening displacements at quarter-point quadratic elements. The results obtained in this paper show a good agreement with other results. The number of elements required is rather small.
Keywords: boundary elements, transversely isotropic materials, dynamic fracture mechanics, three dimensional integral representation.

1 Introduction

There are not many results in the literature for problems of 3-D cracks in transversely isotropic materials, although this kind of materials are of great interest for engineers. Crystal of hexagonal system and fiber reinforced composites show this kind of behavior, provided the dimensions of the crack are much bigger than the fiber diameter.

Kassir and Sih [1] showed 35 years ago that the basic concepts of fracture mechanics for transversely isotropic solids were similar to those of isotropic solids: there is a stress singularity of order $1/\sqrt{r}$ near the crack front and crack opening displacement in the proximity of the crack front have a variation of the type $\sqrt{r}$. Both stress and displacement fields may be described in terms of stress intensity factors (SIFs).

The Boundary Element Method (BEM) is a very useful numerical approach in order to obtain these SIFs. In this paper, a mixed (or dual) formulation of the


Boundary Elements XXVI, C. A. Brebbia (Editor)

BEM is used. This formulation is based on the use of the displacement integral representation for the external boundary and the traction integral representation for the crack surface. Thus, only external boundary and crack surface need to be discretized.

The main disadvantage in the use of the traction integral representation is the additional integration and implementation effort due to the presence of hypersingular and strongly singular kernels. Dominguez *et al*. [2] presented a regularization process in order to deal with this difficulty. This regularization is done prior to any discretization, and the hypersingular and strongly singular integrals appearing in the formulation, are transformed into line and surface integrals, which are at most weakly singular and can be numerically evaluated without difficulty. This formulation can be used for static as well as for dynamic fracture analysis in transversely isotropic solids, as presented by Ariza and Dominguez [3],[4].

Quadrilateral and triangular quadratic elements are used, with quarter-point elements at the crack front. SIFs are evaluated from the quarter-point nodal opening displacement. The transformation of coordinates presented by Telles [5] and a subdivision technique have been used as alternative ways of improving the numerical integration procedure. More accurate results with less CPU time have been obtained with Telles' method. The results presented in this paper show the robustness of the formulation.

2 Formulation

The classical displacement integral equation for an internal point $\mathbf{y}$ of an isotropic or anisotropic elastic body Ω bounded by a regular surface Γ with unit outward normal $\mathbf{n}(\mathbf{x})$ under time harmonic loading and zero body forces can be written as

$$u_l(\mathbf{y},\omega) + \int_\Gamma p^*_{lk}(\mathbf{x},\mathbf{y},\omega)u_k(\mathbf{x},\omega)d\Gamma - \int_\Gamma u^*_{lk}(\mathbf{x},\mathbf{y},\omega)p_k(\mathbf{x},\omega)d\Gamma = 0 \quad (1)$$

for l, k = 1, 2, 3, where u_k and p_k stand for the k component of displacement and traction vectors, respectively, ω is the frequency, and u^*_{lk}, p^*_{lk} are the 3-D elastic time harmonic fundamental solution displacement and traction tensors respectively.

Stress at point $\mathbf{y}$ can be obtained by differentiation of displacement components at that point and introduction of the corresponding strains into the stress-strain relationship.

Thus, the integral representation for the traction components are

$$\begin{aligned} p_l(\mathbf{y},\omega) \quad &+ \int_\Gamma s^*_{lmk}(\mathbf{x},\mathbf{y},\omega)N_m(\mathbf{y})u_k(\mathbf{x},\omega)d\Gamma \\ &- \int_\Gamma d^*_{lmk}(\mathbf{x},\mathbf{y},\omega)N_m(\mathbf{y})p_k(\mathbf{x},\omega)d\Gamma = 0 \end{aligned} \quad (2)$$

where d^*_{lmk} and s^*_{lmk} are linear combinations of derivatives of u^*_{lk} y p^*_{lk}, respectively.

Boundary Elements XXVI, C. A. Brebbia (Editor)

The four fundamental solution kernels in eqns. 1 and 2 can be written as

$$\begin{aligned} u^*_{lk}(\mathbf{x},\mathbf{y},\omega) &= u^R_{lk}(\mathbf{x},\mathbf{y},\omega) + u^S_{lk}(\mathbf{x},\mathbf{y}) \\ p^*_{lk}(\mathbf{x},\mathbf{y},\omega) &= p^R_{lk}(\mathbf{x},\mathbf{y},\omega) + p^S_{lk}(\mathbf{x},\mathbf{y}) \\ d^*_{lmk}(\mathbf{x},\mathbf{y},\omega) &= d^R_{lmk}(\mathbf{x},\mathbf{y},\omega) + d^S_{lmk}(\mathbf{x},\mathbf{y}) \\ s^*_{lmk}(\mathbf{x},\mathbf{y},\omega) &= s^R_{lmk}(\mathbf{x},\mathbf{y},\omega) + s^S_{lmk}(\mathbf{x},\mathbf{y}) \end{aligned} \tag{3}$$

where $\mathrm{u}^R_{lk}(\mathbf{x},\mathbf{y},\omega)$, $\mathrm{p}^R_{lk}(\mathbf{x},\mathbf{y},\omega)$, $\mathrm{d}^R_{lmk}(\mathbf{x},\mathbf{y},\omega)$ and $\mathrm{s}^R_{lmk}(\mathbf{x},\mathbf{y},\omega)$ are regular functions of r which tend to zero as ω does, and $u^S_{lk}(\mathbf{x},\mathbf{y})$, $p^S_{lk}(\mathbf{x},\mathbf{y})$, $d^S_{lmk}(\mathbf{x},\mathbf{y})$ and $s^S_{lmk}(\mathbf{x},\mathbf{y})$, correspond to the static counterpart of u^*_{lk}, p^*_{lk}, d^*_{lmk} and s^*_{lmk}, respectively. The four static terms present singularities of the type r^{-1}, r^{-2}, r^{-2} and r^{-3}, respectively, when $r \to 0$.

In a static problem, with no frequency dependency, only the static part of the fundamental solution is used, whereas in the dynamic case, the regular part have to be added. Explicit expressions of $u^S_{lk}(\mathbf{x},\mathbf{y})$ and $\sigma^S_{lmk}(\mathbf{x},\mathbf{y})$ for three dimensional transversely isotropic materials were obtained by Pan and Chou [6].

The expressions for d^{*S}_{lmk} coincide, except for a change of sign, with σ^S_{lmk}. This change of sign is due to the different differentiation point: integration point (x) for σ^S_{lmk} and collocation point for d^{*S}_{lmk}. Explicit expressions for s^{*S}_{lmk}, can be obtained by differentiation and combination of Pan and Chou's expressions of p^S_{lk}. They can be found in Ariza and Dominguez [3].

The frequency dependent regular part of the fundamental solution u^{*R}_{lk} can be obtained by subtracting the static fundamental solution from the time harmonic fundamental solution for general anisotropic solids $u^*_{lk}(\mathbf{x},\mathbf{y},\omega)$ obtained by Wang and Achenbach [7].

Taking into account the fundamental solution kernels decomposition in eqn. 3, the equations can be written for a boundary point following the same steps as in the static case. The displacement integral equation (1) becomes

$$\begin{aligned} &c_{lk}(\mathbf{y})u_l(\mathbf{y},\omega) + \int_\Gamma p^{*S}_{lk}(\mathbf{x},\mathbf{y})u_k(\mathbf{x},\omega)d\Gamma - \int_\Gamma u^{*S}_{lk}(\mathbf{x},\mathbf{y})p_k(\mathbf{x},\omega)d\Gamma \\ &+ \int_\Gamma p^{*R}_{lk}(\mathbf{x},\mathbf{y},\omega)u_k(\mathbf{x},\omega)d\Gamma - \int_\Gamma u^{*R}_{lk}(\mathbf{x},\mathbf{y},\omega)u_k(\mathbf{x},\omega)d\Gamma = 0 \end{aligned} \tag{4}$$

The traction integral equation (2) becomes

$$\begin{aligned} \frac{1}{2}p_l(\mathbf{y},\omega) + \int_\Gamma \Big\{ & s^S_{lmk}N_m \left[u_k(\mathbf{x},\omega) - u_k(\mathbf{y},\omega) - u_{k,h}(\mathbf{y},\omega)(x_h - y_h)\right] \\ & - d^S_{lmk}N_m \left[p_k(\mathbf{x},\omega) - p_k(\mathbf{y},\omega)\right] \Big\} d\Gamma \\ & + \left[u_k(\mathbf{y},\omega)I_{lk} + u_{k,h}(\mathbf{y},\omega)J_{lhk} + p_k(\mathbf{y},\omega)K_{lk}\right] \\ + \int_\Gamma \left\{ s^R_{lmk}N_m u_k(\mathbf{x},\omega) - d^R_{lmk}N_m p_k(\mathbf{x},\omega) \right\} d\Gamma &= 0 \end{aligned} \tag{5}$$

Eqn. (5) is obtained after regularization of integrals containing the static (singular) parts, following the same approach proposed by Ariza and

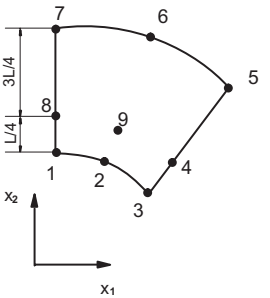

Figure 1: Nine node quarter-point quadratic element.

Dominguez [3] for transversely isotropic materials and by Dominguez *et. al* [2] for isotropic materials. The first term of the traction series expansion and the first two terms of the displacements expansions at collocation point, are subtracted and added back. The integrals of the singular added back terms are transformed into regular or weakly singular integrals by using Stoke's theorem. Explicit expressions of I_{lk}, J_{lhk} and K_{lk} can be seen in Ariza and Dominguez [3].

3 Discretization

The discretization and implementation effort is greatly simplified by the use of the present mixed BE approach (see Ariza and Dominguez,[3], [8]). Only the crack surface and the external boundary need to be discretized. The traction BIE is used for collocation points that may be assumed to be on any of the two crack surfaces, whereas the classical BIE is written on the nodes of the external boundaries, when they exist.Thus, the Crack Opening Displacement (COD) is chosen as the basic variable on the crack, whereas displacements and tractions are the variables of he external boundaries. No collocation at all is needed for the nodes at the crack front, where COD=0.

Standard six-node or nine-node quadratic elements are used, except for those with one side at the crack front which are quarter-point elements (Figure 1). These elements are able to reproduce the $\sqrt{r}$ behaviour of the displacements in the vicinity of the crack front (see [9], [10]).

Following the idea of Gallego and Dominguez [11] for two dimensions, the collocation is not done at the contour nodes, i.e. at ξ_1, $\xi_2 = \pm 1$, but at certain points close to the nodes, inside the element (ξ_1, $\xi_2 = \pm 0.75$). Notice that the elements used are continuous, as only the collocation points are shifted to the interior of the element.

As a consequence of the collocation strategy, one may have as many equations for each nodal component as elements contain the node. These equations are added up to yield only one per nodal component. It is worth to notice that this Multiple Collocation Approach (MCA) is only used for the nodes of the crack surface, where the traction BIE is used. It is also important to mention that the regulariza-

tion process of the static part of the fundamental solutions is only applied over a part of the surface Γ close to the collocation point, whereas the original expressions of the integrals are used in the rest of the boundary, where they are non singular.

Thus, the expression to be discretized into boundary elements is

$$\begin{aligned}\frac{1}{2}p_l(\mathbf{y},\omega) + \int_{\Gamma_0} \big\{ & s^S_{lmk} N_m \left[u_k\left(\mathbf{x},\omega\right) - u_k(\mathbf{y},\omega) - u_{k,h}(\mathbf{y},\omega)(x_h - y_h)\right] \\ & - d^S_{lmk} N_m \left[p_k\left(\mathbf{x},\omega\right) - p_k(\mathbf{y},\omega)\right] \big\}\, d\Gamma \\ & + \left[u_k(\mathbf{y},\omega) I^0_{lk} + u_{k,h}(\mathbf{y},\omega) J^0_{lhk} + p_k(\mathbf{y},\omega) K^0_{lk}\right] \\ + \int_{\Gamma-\Gamma_0} \big\{ & s^S_{lmk}(\mathbf{x},\mathbf{y},\omega) N_m(\mathbf{y}) u_k(\mathbf{x},\omega) - d^S_{lmk}(\mathbf{x},\mathbf{y},\omega) N_m(\mathbf{y}) p_k(\mathbf{x},\omega) \big\}\, d\Gamma \\ & + \int_{\Gamma} \big\{ s^R_{lmk} N_m u_k(\mathbf{x},\omega) - d^R_{lmk} N_m p_k(\mathbf{x},\omega) \big\}\, d\Gamma = 0.\end{aligned} \tag{6}$$

where Γ_0 is the element containing the collocation point, and $\Gamma - \Gamma_0$ is the rest of the boundary. Regarding the numerical integration of the nearly singular and weakly singular kernels, the subdivision technique and the well known transformation of coordinates proposed by Telles [5] have been considered. The results are more accurate, the approach is more robust and lees CPU time consuming when Telles transformation and a suitable number of Gauss points are used.

4 Stress intensity factors evaluation

According to the work of Kassir and Sih [1], the SIFs can be obtained from the COD near the crack front for the static case as well as for the dynamic one. Assuming that *z* is the material axis of symmetry perpendicular to the crack plane and the *t*-axis is tangent to the crack front line at the point where a node is located (Figure 2), the SIFs components at this point can be written in terms of the crack opening displacements at the quarter-point node as:

$$\begin{aligned} K_I &= \sqrt{\frac{\pi}{2L}} \Delta u_z \frac{\beta_1}{\frac{m_1}{1+m_1} - \frac{m_2}{1+m_2}} \\ K_{II} &= \sqrt{\frac{\pi}{2L}} \Delta u_n \frac{C_{44}\left(\sqrt{n_2} - \sqrt{n_1}\right)(1+m_1)(1+m_2)}{(m_2 - m_1)\sqrt{n_1 n_2}} \\ K_{III} &= \sqrt{\frac{\pi}{2L}} \Delta u_t \frac{C_{44}}{\sqrt{n_3}} \end{aligned} \tag{7}$$

where L is the quarter-point element width, n_1 and n_2 are the two solutions of the quadratic characteristic equation of the material properties.

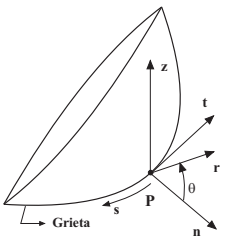

Figure 2: Local coordinates at crack boundary point P.

5 Numerical results

In the following two different crack problems in transversely isotropic media are analyzed.

A penny shaped crack under time harmonic loading in unbounded transversely isotropic media is studied first. The second problem corresponds to a prismatic bar with a surface crack under uniform static loading. This problem is particularly demanding because there is flexure and non-symmetric behavior in the body. The problem is used for the analysis of different integration schemes in relation to the efficiency and accuracy of the BE approach.

5.1 Penny shaped crack in unbounded domain

A penny shaped crack is located in a plane perpendicular to the material axis of symmetry of a transversely isotropic unbounded domain. The considered materials are a graphite-epoxy (C_{11}=13.92 GPa; C_{33}=160.7 GPa; C_{12}=6.92 GPa; C_{13}=6.44 GPa; C_{44}=7.07 GPa and ρ=1578 kg/m^3) and an isotropic material (G=100 GPa, ν=0.3). The crack is under the effect of time harmonic quasi-longitudinal waves propagating along the material axis of symmetry. Two BE meshes are used for the present analysis (Figure 3.a). In both figures all the elements are quadrilateral nine-node elements with the mid-node of the external elements at one quarter of their width. The mesh in Figure 3.b is used for high frequency values. These meshes satisfy the condition that the largest element length in the crack $L \leq \lambda/10$, λ being the smallest wave length in the crack plane, that takes place for the largest frequency analyzed with each mesh.

Using the quarter-point COD and eqn. 7, the mode-I SIF for a frequency range $0 \leq K_T a \leq 2$. Figure 4 shows a comparison of the present BE results with those obtained by Tsai [12] . The SIF is normalized by the static value due to an internal pressure with the same amplitude of the dynamic pressure. The agreement between both sets of results is very good.

Results obtained with the present approach for a wider frequency range are shown in Figure 5 (note that the first part of this figure is the same as Figure 4). No previous results for this frequency range are known by the authors.

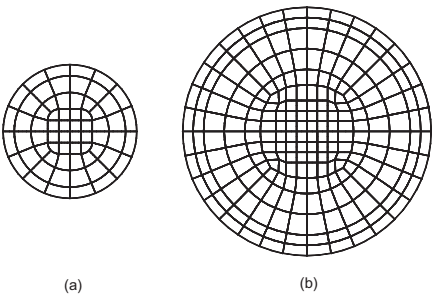

Figure 3: Boundary element discretization of a penny shaped crack in infinite domain: (a) low frequency analysis; (b) high frequency analysis.

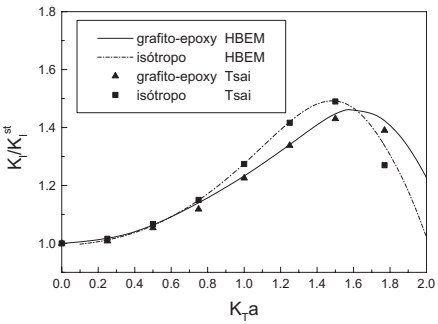

Figure 4: Mode-I dynamic SIF for penny shaped crack (low frequency range).

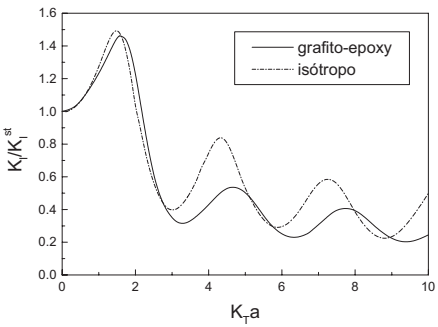

Figure 5: Mode-I dynamic SIF for penny shaped crack (large frequency range).

5.2 Square bar with a corner quarter-circle crack under uniform traction

The problem geometry for this case is shown in Figure 6.a. The BE mesh used is shown in Figure 7. A uniform traction σ is prescribed on the ends of the bar. Besides the two materials of the previous example, a laminate composite with the

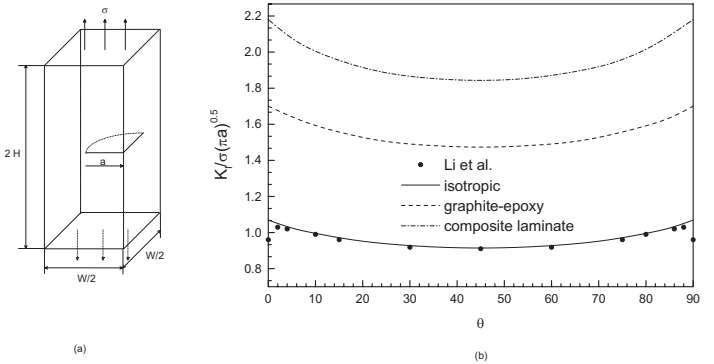

Figure 6: Rectangular bar with a semi-circular surface crack. (a) Geometry (b) SIF mode-I.

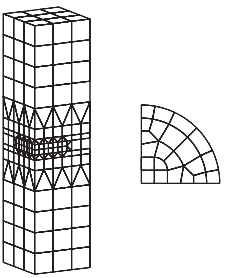

Figure 7: BE discretization of one half of a rectangular bar with a semi-circular surface crack.

following properties is also considered:C_{11}=5.37 GPa, C_{33}=251.168 GPa, C_{12}=1.34 GPa, C_{13}=3.35 GPa and C_{44}=5 GPa. The distribution of K_I along the crack front as a function of θ is shown in figure 6.b for the same three materials studied in the previous example. The K_I variation with θ is quite similar for the three analyzed materials. These values are smaller as the material is more isotropic. The results for the isotropic case are compared with those obtained by Li *et al.* [13] using a symmetric integral equation formulation. The agreement is very good.

Results for the most anisotropic material considered (laminate composite) are obtained for different discretizations of the crack, with different number of elements at the crack front and different aspect ratio (Figure 8). These results show the robustness of the approach, as there is very little mesh dependency.

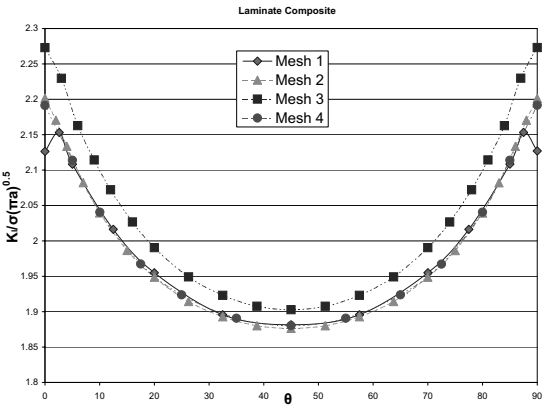

Figure 8: Results for different discretizations.

6 Conclusions

A single-domain BE formulation for the static and dynamic analysis of fracture problems in three-dimensional transversely isotropic solids has been presented in this paper. Time harmonic loading conditions are considered.

The present approach allows for the general analysis of cracks in transversely isotropic domains with little effort. Discretization is reduced to the crack surface, where the number of elements is rather small, and the external surface.

Acknowledgements

This work was support by the Ministerio de Ciencia y Tecnologa of Spain (DPI2000-1217-C02-01 and DPI2001-2377-C02-01). The financial support is gratefully acknowledged.

References

[1] Kassir, MK. and Sih, GC., Three-dimensional stresses around elliptical cracks in transversely isotropic solids, *Engng. Fract. Mech.* **1** (1968) 327–345.

[2] Dominguez, J., Ariza, MP., and Gallego, R., Flux and traction boundary elements without hypersingular or strongly-singular integrals, *Int. J. Numer. Meth. Engng.* **48** (2000) 111–135.

[3] Ariza, MP., and Dominguez,J., Boundary element formulation for 3-D transversely isotropic cracked bodies, *Int. J. Numer. Meth. Engng.* (In press).

[4] Ariza, M.P. and Dominguez,J., Dynamic BE analysis of 3-D cracks in transversely isotropic solids, *Computer Methods in Appl. Mech. Engrg.*, (2004), (In press)
[5] Telles, J.C.F., A self-adaptive coordinate transformation for efficient numerical evaluation of general boundary element integrals, *Int. J. Numer. Meth. Engng.* **24** (1987) 959–973.
[6] Pan, YC. and Chou, TW., Point force solution for an infinite transversely isotropic solid, *J. Appl. Mech.* **43** (1976) 608–612.
[7] Wang, CY., and Achenbach, JD., 3-D Time-harmonic elastodynamic green's functions for anisotropic solids, *Proc. Roy. Soc. London* **A449** (1995) 441–458.
[8] Ariza, MP., and Dominguez, J., General BE approach for three-dimensional dynamic fracture analysis, *Engng. Anal. Boundary Elem.* **26** (2002) 639–651.
[9] Saez, A., Ariza, MP., and Dominguez, J., Three-dimensional fracture analysis in transversely isotropic solids, *Engng. Anal. Boundary Elem.* **20** (1997) 287–298.
[10] Ariza, MP., Saez, A., and Dominguez, J., A singular element for three-dimensional fracture mechanics analysis, *Engng. Anal. Boundary Elem.* **20** (1997) 275–285.
[11] Gallego, R., and Dominguez, J., Hypersingular BEM for transient elastodynamic, *Int. J. Numer. Meth. Eng.* **39** (1996) 1681–1705.
[12] Tsai, YM., Dynamic penny-shaped crack in a transversely isotropic material, *Eng. Fract. Mech.* **31** (1988) 977–984.
[13] Li, S., Mear, ME., Xiao, L. Symmetric weak-form integral equation method for three-dimensional fracture analysis. *Computer Methods in Applied Mechanics and Engineering* 1998; **151**:435–459.

Boundary Elements XXVI, C. A. Brebbia (Editor)